Grid Integration of a Novel Linear-generator-based Wave Power Conversion System

Renqi Guo
School of Engineering
Lancaster University
Lancaster, UK
r.guo2@lancaster.ac.uk

Yueqi Wu
School of Engineering
Lancaster University
Lancaster, UK
y.wu31@lancaster.ac.uk

Xiandong Ma
School of Engineering
Lancaster University
Lancaster, UK
xiandong.ma@lancaster.ac.uk

George Aggidis
School of Engineering
Lancaster University
Lancaster, UK
g.aggidis@lancaster.ac.uk

Nan Zhao
School of Engineering
Lancaster University
Lancaster, UK
nan.zhao@lancaster.ac.uk

***Abstract*—Wave Energy Converter (WEC) systems harness kinetic energy from ocean waves, with the power take-off (PTO) system facilitating the conversion to electrical power. While hydraulic systems are commonly used PTOs, linear generators (LGs) are promising alternatives due to their direct energy conversion, high efficiency, and environmental benefits. Since waves propagate in multiple directions, multi-axis WEC has superiority in more consistent power generation than traditional single-axis WECs. This paper will focus on integrating multi-axis WEC with the AC grid. A novel LG-based power conversion system is proposed for the six-axis WEC, aimed at facilitating grid integration and support. Additionally, the integration of a battery energy storage system (BESS) helps stabilize the DC link voltage and enables grid-forming capabilities. This research also discusses the placement of BESS at either the DC link or AC side of the system. Although BESS on the AC side can provide sufficient grid support, challenges in maintaining the appropriate DC link voltage of VSC arise when WEC power exceeds converter ratings or does not match the grid demand. Our analysis recommends the DC link as the preferable BESS location, with the size of the BESS being a critical factor in smoothing power fluctuations and maintaining voltage stability.**

Keywords—wave energy converter, grid-forming converter, battery energy storage system, grid integration

I. INTRODUCTION

As climate concerns become serious, renewable energy has been a popular topic during the past decades. Renewable energy can be converted into electricity through various topologies, significantly reducing carbon emissions when compared with traditional generator-based power plants. European countries stand to benefit significantly from the utilization of renewable energy sources to achieve the target of net-zero carbon by 2030 [1]. For coastal countries, wave energy plays an important role in their renewable plans. To harness the kinetic energy of the wave and transfer it into electricity, wave energy converter (WEC) has been investigated for many years. Many literatures have focused on single-direction WEC, while the wave motion has more than six degrees of freedom [2]. Therefore, WEC with the operation at multiple axes can absorb more power than that with a single axis. Technologically Advanced Learning Ocean System (TALOS) was proposed by researchers at Lancaster University [3] and was further developed recently [4], which is a point-absorber type WEC and has six axes Power Take-Off (PTO) system. The prototype and experimental environment of TALOS are illustrated in Fig. 1. As can be seen, the hull connects the heavy ball with springs. If a hydraulic system is used as PTO, the relative motion between the ball and hull can produce force to pump the hydraulic cylinders to generate fluid which drives the hydraulic motor to generate electricity. However, there are some drawbacks and limitations of using a hydraulic system as PTO. For instance, there is a risk that the hydraulic liquid may leak, causing environmental damage [5]. Additionally, the process of hydraulic systems involves two energy conversion stages, including the conversion from mechanical energy to hydraulic energy and the reconversion from hydraulic energy into mechanical energy to drive the motor. This is more complex when compared with other PTO systems, such as permanent magnet linear generator (PMLG) [6]. PMLG has only one energy conversion stage, transforming mechanical energy into electricity directly. The direct conversion also means less need for maintenance and high efficiency [7]. This paper focuses on a six-PMLG based power conversion system.

To integrate renewables into the AC grid, power electronics are crucial. Since the AC side normally requires a stable operation with acceptable frequency. For example, back-to-back voltage source converters (VSCs) are commonly used in renewable integration, which can decouple the fluctuated renewable resource from the stable AC grid [8]. Since the grid code requires renewable farms to participate in frequency response [9], the grid-forming (GFM) capability of future renewable power plants has drawn more and more attention. Authors in [10] investigated the control of back-to-back VSC in the WEC system, but the priority was to increase the efficiency of the PTO system to maximize the power output. In [11], the researchers also used the back-to-back structure, but they focused on the WEC floater related system, the estimator and PTO control, not investigating the grid integration of WEC. Authors in [12] proposed Lyapunov-based nonlinear controllers to solve various conflicts in the power train of the WEC system, and a supercapacitor was used as an energy storage to stabilize DC voltage. To smooth the output power to realize a better grid integration, the battery energy storage system (BESS) in [13] and supercapacitor in [14] were adopted in their scheme; however, they are not designed for grid support due to the constraints of the control of grid-side VSC. Most researchers focus more on grid-following (GFL) controlled systems. However, some literature developed the GFM-

based WEC system to support the grid actively. In [15], a droop controller was applied to help the grid realize the capability of frequency response. Authors in [16] proposed a multi-mode control for converter, to actively switch mode (grid feeding, grid support and grid forming) according to the grid conditions. However, they consider their storage system to be ideal without the size optimization and location comparison.

The existing literatures focus more on maximum utilization of WEC, either in the aspects of mechanical or electrical control of WEC systems. However, few of them investigate the GFM capability of the WEC system. This paper proposes a GFM-based WEC scheme. The first contribution of this paper is the integration of six-PMLG based WEC system with the experimental TALOS data as input. This integration facilitates the assessment of the grid-forming capability of the proposed GFM-based WEC system, providing adequate grid support in terms of frequency response and voltage stability. Both constant power mode and maximum power point tracking (MPPT) mode are tested. In addition, a detailed discussion on the location of BESS indicates that the DC link is a better choice for BESS. This placement not only smooths the power output of WEC but also stabilizes the DC link voltage. This paper also contributes to the investigation into the optimal size of the Battery Energy Storage System (BESS), considering both power smoothing and the provision of frequency response simultaneously.

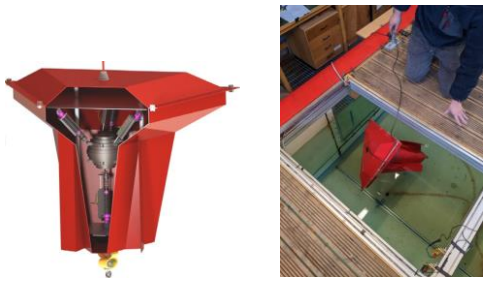

(a) (b)

Fig. 1. Prototype of TALOS [3]. (a) designed prototype; (b) experimental environment

The paper is organized as follows: Section II introduces the modelling of the WEC system; Section III presents the simulation results of the WEC system, which shows the GFM capability; Section IV compares the different locations of BESS and optimizes the size of the battery; Section V draws the conclusion.

II. Power Conversion System Modelling

A. Overall WEC System

The proposed power conversion system primarily comprises six PMLGs, a BESS and a grid-side VSC. In this system, TALOS absorbs the kinetic energy, which drives the PMLGs to generate electrical power. The six PMLGs are connected to the DC link via passive rectifiers, and there is a DC/DC converter between the battery and the DC link. The function of BESS is to provide/absorb the required power for both smoothing and frequency response. Moreover, it can also stabilize the DC link voltage by controlling the DC/DC converter. The grid-side converter is a GFM-controlled VSC, which injects the required power into the grid while supporting the power system with its grid-forming capabilities. From the grid side, the GFM controlled VSC can be regarded as a voltage source, and this allows the system to actively provide frequency and voltage support. Fig. 2 illustrates the structure of the system.

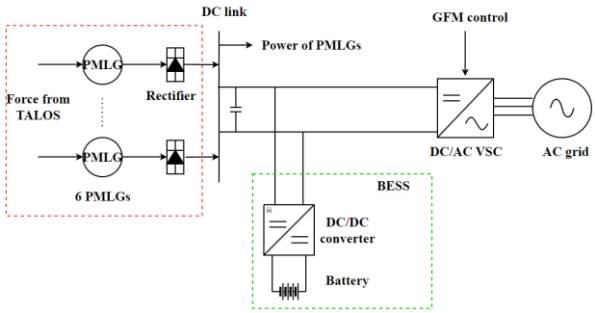

Fig. 2. WEC system with BESS

B. PMLG and WEC

There are some conditions for the simplification of WEC experiment. The TALOS has six dampers, and normally the six motions are considered, namely yaw, heave, pitch, sway, roll and surge. This is illustrated in Fig. 3. In our test, six PTOs are used for capturing the forces of these six motions. As a result, six PMLGs are implemented. Through the experiment, TALOS has two symmetries for the *x* and *y* axes, which means the force from the motions of pitch and roll are the same (PTO 2 and 3), and PTO for sway and surge have the same response as well (PTO 5 and 6) [3].

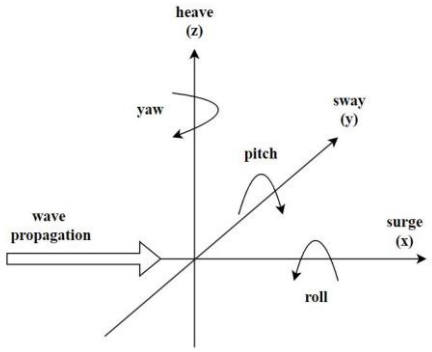

Fig. 3. Six motions of TALOS [3]

The PMLG basically has a similar design concept and analysis as a traditional permanent magnet synchronous generator (PMSG) [17]. The main difference is the motion of the rotor. The PMSG has a rotational rotor with constant speed, while the PMLG's rotor, named translator is not rotational and has a continuously changing speed. The force from TALOS drives the translator of PMLG to generate electricity.

C. Control of DC/AC VSC

1) Active Power and Reactive Power Control

Different from grid-following (GFL) controlled VSC, the system with GFM can form the grid and be regarded as a voltage source from the perspective of the grid. In this paper, one of the most popular GFM topologies is implemented, named virtual synchronous generator (VSG). VSG was first proposed by Beck and Hesse in 2007 [18]. The key of VSG is the swing equation, which mimics the behaviour of a traditional synchronous generator (SG). The voltage angle is determined by (1), while the voltage magnitude is controlled by reactive power which is shown in (2) [19].

$$J\frac{d\Delta\omega_{vsg}}{dt} = P_{ref} - P_e - K_d * \Delta\omega_{vsg} \quad (1)$$

$$\omega_{vsg} = \Delta\omega_{vsg} + \omega_g \quad (2)$$

$$E = V_{ref} - K_q * (Q_{ref} - Q_e) \quad (3)$$

where J is the virtual inertia of VSG; K_d is the damping factor; P_{ref} and P_e are reference active power and output active power respectively; $\Delta\omega_{vsg}$ represents the frequency change of VSG ;ω_{vsg} and ω_g are the frequency of VSG and grid; E , V_{ref} , K_q , Q_{ref} and Q_e are the virtual electric potential, reference voltage for the converter, reactive power gain, reference reactive power and output reactive power of VSG.

Note that the active power reference for VSG has two choices depending on the requirement of the grid. If the grid allows the WEC system to operate at maximum power point tracking (MPPT) mode, the P_{ref} will be the direct power output of PMLGs. However, the power of PMLGs has fluctuations due to the characteristics of waves. To smooth the power injected into the AC grid, a filter is designed for this purpose.

$$P_{ref} = \frac{\omega_f}{s + \omega_f} * P_{\lg} \quad (4)$$

In (4), P_{lg} represents the output power of PMLGS and ω_f is the cutoff frequency of the low-pass filter. With the filter, the fluctuations of the power can be reduced. Normally, the cutoff frequency should be much smaller than the nominal frequency of the grid [20]. In this paper, ω_f is selected as 10, resulting the filter has a time constant as 0.1s. When the grid requires the WEC system to operate at constant power, then the P_{ref} is set to be constant and BESS can automatically smooth the power difference between P_{lg} and P_{ref}.

The virtual impedance aims at generating reference voltage to the voltage controller for the converter. It also provides a link between VSG and the grid. X_v is the virtual impedance of VSG and r_v is virtual resistance. u_o and i are the output voltage and current of VSG respectively. This relationship is expressed in (5).

$$u_o = E - i * (r_v + jX_v) \quad (5)$$

2) Voltage and Current Controller

VSG control contains an outer voltage controller, an inner current controller and pulse-width modulation (PWM), which controls the dynamics of the converter. The voltage controller is introduced by (6) and (7), while the current controller is not included in this part due to its same structure as voltage controller.

$$i^*_{dvsc} = K_{pv}(u^*_{od} - u_{od}) + K_{iv}\int(u^*_{od} - u_{od}) - \omega_{vsg}c_f u_{oq} \quad (6)$$

$$i^*_{qvsc} = K_{pv}(u^*_{oq} - u_{oq}) + K_{iv}\int(u^*_{oq} - u_{oq}) + \omega_{vsg}c_f u_{od} \quad (7)$$

where i^*_{dvsc} and i^*_{qvsc} are the reference current for the current controller, which is produced by the voltage controller; K_{pv} and K_{iv} are the PI gains of the voltage controller; c_f is the filter capacitance of VSG.

The power output equations in the DQ-frame are (8) and (9). The output power P_e and Q_e are also respectively the feedback values used in active power control (1) and reactive power control (3) at the same time.

$$P_e = \frac{3}{2}(u_{od}i_d + u_{oq}i_q) \quad (8)$$

$$Q_e = \frac{3}{2}(-u_{od}i_q + u_{oq}i_d) \quad (9)$$

D. Control of DC/DC Converter

The function of the BESS is to compensate the instantaneous power difference between the desired power injected into the AC grid and the direct power output of PMLGs, i.e. smoothing the power output for stable operation of the grid. Since the PWM generation requires the participation of DC link voltage, a stable DC voltage is beneficial for the quality of VSC output. Therefore, the second target of the battery is to stabilize the DC link voltage. The control diagram of the DC/DC converter is shown in Fig. 4, which is PI control that regulates the DC voltage with the reference voltage

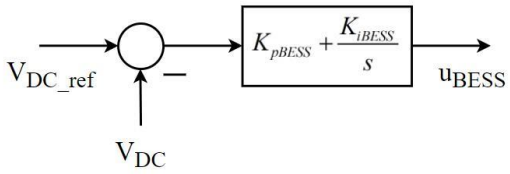

Fig.4. Control of DC/DC converter

III. Results of Grid Support

The TALOS was tested in laboratory and experimental data about torque, speed and force were acquired. Since this work focuses on the integration of the WEC system into the grid, the force is the only experimental data that has been used. As mentioned before, due to the symmetry of motions, PTO 2 and 3 have the same force, and PTO5 and 6 have the same case. Fig. 5 shows the wave surface elevation, PTO forces and power output of six individual PMLGs from the tested TALOS during a short period.

A. Frequency Response

The PMLG-based WEC system was built on MATLAB Simulink. The system voltage is 10 kV, and detailed parameters can be found in Table I. Parameters are calculated based on the principles of converter design illustrated in [21], with the combination of VSG theory. The system operates at 50 Hz, and frequency response performance is tested first. From 1s, the grid experiences a frequency drop event, Fig. 6 shows the results of the proposed WEC system. From Fig. 6 (a), it can be seen that the DC link voltage maintains almost constant. Fig. 6 (b) shows the power output from BESS (P_b), PMLGs (P_{lg}) and the actual power injected into the AC grid (P_{ac}) under MPPT mode. With the help of the designed filter in (4), the curve of P_{ac} is very smooth. After 1s, the GFM control allows the BESS to provide the additional power for frequency response with approximately 0.3 MW. When the system operates in

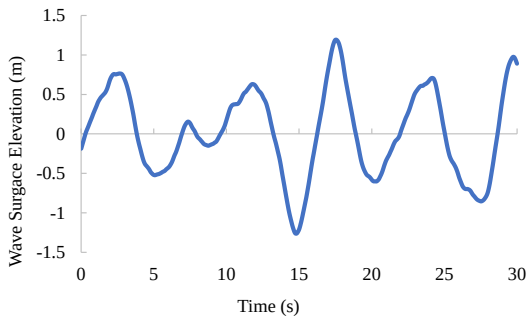

(a)

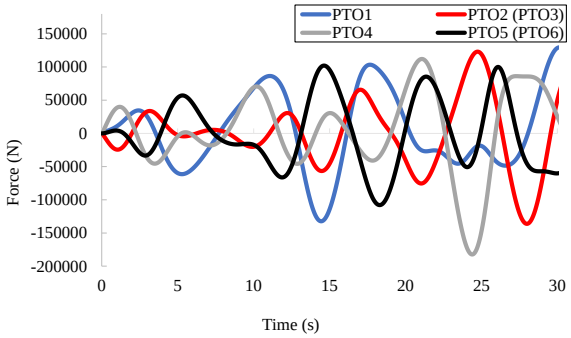

(b)

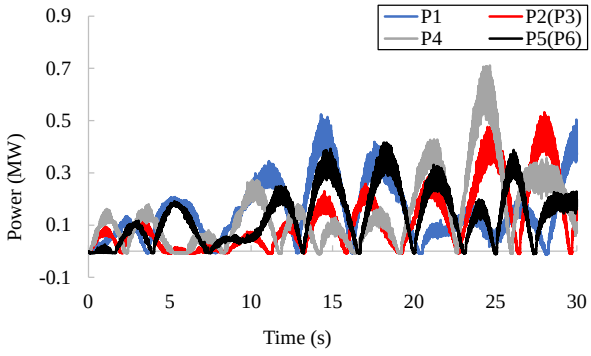

(c)

Fig.5. Results from experiments. (a) wave profile, (b) generated forces, (c) individual power of six PMLGs.

constant power output mode, the results are shown in Fig. 6 (c). It is clear that the power output of VSC is constant without fluctuations, and it can perfectly participate in frequency response as well. The BESS balances the power difference between P_{ref} and P_{lg}.

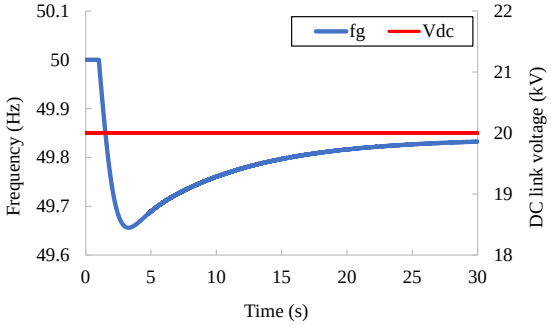

(a)

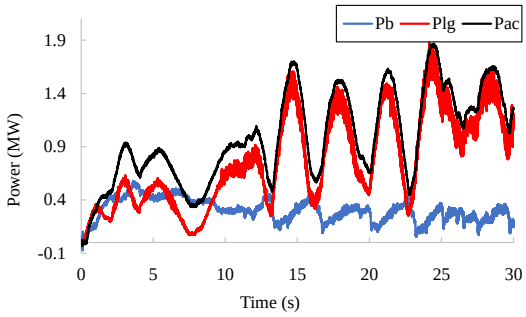

(b)

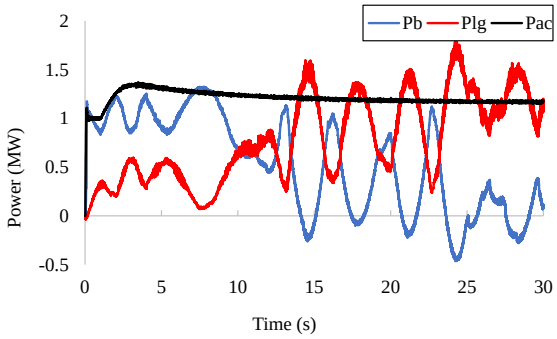

(c)

Fig.6. Frequency response under different modes. (a) frequency and DC voltage change, (b) MPPT mode, (c) constant power mode.

B. *Voltage Support*

When the system frequency maintains constant and the voltage drops from 1.0 p.u. to 0.9 p.u. at 3s, the reactive power from VSC is observed. The active power output is also plotted as a comparison with part A.

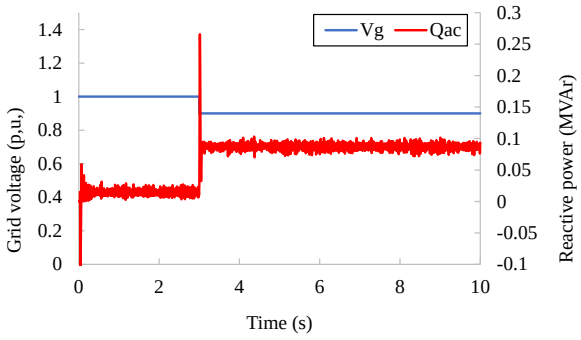

(a)

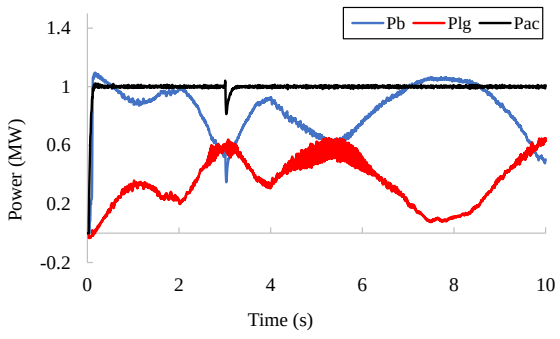

(b)

Fig.7. Results of voltage support. (a) voltage change and reactive power response, (b) active power.

From Fig. 7, it is obvious that the GFM-controlled VSC effectively generates reactive power to support the voltage drop; the active power output is barely influenced.

IV. Size and Location of BESS

A. Size of BESS

From the curve of P_b in Fig. 6 (b), Fig. 6 (c) and Fig. 7 (b), the factors that determine the size of BESS include the operation mode (MPPT or constant power output) and the frequency response requirement, and it is irrelevant to the voltage support. According to the deduction in [13], the power output of a PMLG can be expressed as (10).

$$P = \frac{3}{4}(E_p I_p \cos(2\omega_t t) + E_p I_p) \quad (10)$$

where E_p and I_p are the output phase voltage and current of PMLG, ω_t is the speed of the translator of the generator.

According to (10), the average power of PMLG can be acquired as $\frac{3}{4}E_p I_p$. Therefore, from the perspective of smoothing the power output of PMLGs, the BESS should compensate for the sinusoidal part of (10), which has a peak value as the average power. This is represented by (11).

BESS should also provide power for frequency response. If the frequency response reacts to $(50\pm\Delta f)$ Hz, this part of power can be expressed as (12). Summing up (11) and (12), the overall capacity of BESS can be determined by (13). For example, the rating of PMLGs in this study is 2 MW. To operate and provide frequency support between 49.5 to 50.5 Hz, considering K_d and J in the paper, the total capacity of a BESS should be around 2.5 MW to maintain a constant power output. Note that this is an estimation based on the deduced equations; The optimum energy management system of BESS considering the state of charge (SoC) will be implemented in future work for more accurate sizing.

$$P_{b1} = \frac{3}{4}E_p I_p \cos(2\omega_t t) \quad (11)$$

$$P_{b2} = J\frac{d\Delta f}{dt} + K_d * \Delta f \quad (12)$$

$$P_b = \frac{3}{4}E_p I_p \cos(2\omega_t t) + J\frac{d\Delta f}{dt} + K_d * \Delta f \quad (13)$$

TABLE I. System Settings

Symbol	Name	Value
S_n	System nominal apparent power	2 MVA
V_{base}	Base voltage	10 kV
r_f	Filter resistance	0.1 pu
l_f	Filter inductance	0.5 pu
C_f	Filter capacitance	42 μF
C_{dc}	DC link capacitance	0.02 F
ω_{ref}	Reference frequency	314.159 rad/s
J	Inertia	2600 Kg ∗ m^2
K_d	Droop/damping gain	169000
K_q	Reactive power droop	0.01
ω_c	cutoff frequency of filter	10 rad/s
r_v	Virtual resistance	0.4 pu
l_v	Virtual inductance	0.25 pu
r_g	line resistance	0.2 pu
l_g	Line inductance	0.8 pu
K_{pc}/K_{ic}	Current controller P/I	0.161/19.54
K_{pv}/K_{iv}	voltage controller P/I	9.244/1327
t_s	Sampling time of simulation	$1.481e^{-5}$s
φ_{PM}	Flux of PMLG	40Wb
γ	Polar pitch	0.1m
R_s	Stator resistance	0.26 Ohm
L_s	Stator inductance	30 mH

B. Location of BESS

In addition to the scheme proposed in Fig. 2, there is another structure of the WEC system, where the BESS is at the AC side and the grid-side VSC of the WEC system adopts GFL control. Different from GFM, the GFL controls the DC link voltage and reactive power of the WEC system, while the BESS is at the AC side.

The system diagram is illustrated in Fig. 8. The simulation tests the same case of frequency response in Section III, and the results can be found in Fig. 9.

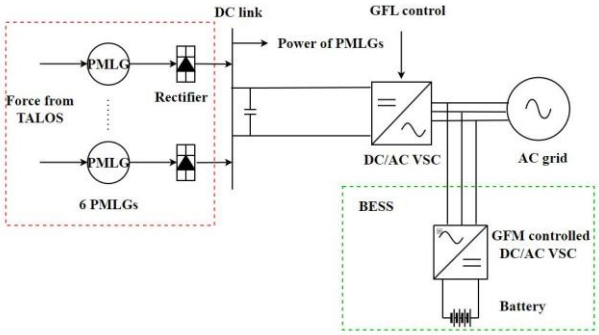

Fig.8. Scheme with BESS at AC side

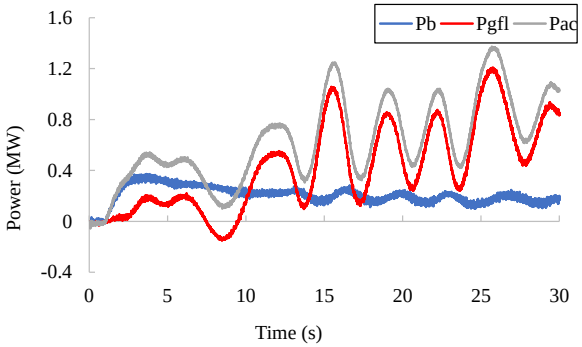

(a)

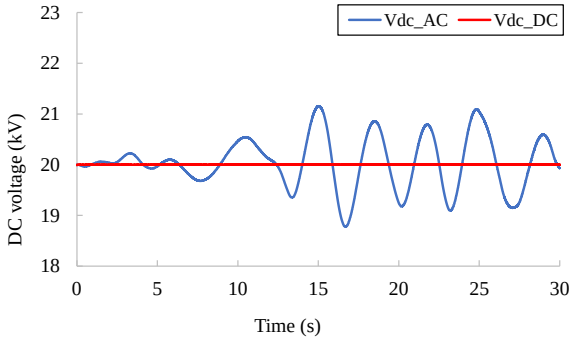

(b)

Fig. 9. Results with BESS at AC side (MPPT mode). (a) active power (b) DC link voltage comparison with different locations of BESS.

Results of Fig. 9 (a) show that the GFL control (P_{gfl}) can smooth the power output of PMLGs and BESS (P_b) supports this as well. Note that MPPT mode is used in this case. The overall power (P_{ac}) injected into the AC grid is acceptable. However, the DC link voltage has large fluctuations without the regulation of additional energy sources. From Fig.9 (b), V_{dc_AC} is the DC voltage when BESS is at DC side, and V_{dc_DC} is the case with BESS at DC link. Although this fluctuation can be reduced by enlarging the capacitance of the DC capacitor, this will lead to a low efficiency for power conversion from the DC link to the AC grid. Also, there is a risk that the PWM control of the converter may get saturation and instability might occur if the voltage is lower than twice of the grid voltage [21]. Therefore, there exists a compromise between the power tracking time and DC link voltage stability.

Therefore, the DC link is a better location for BESS in the WEC system when compared with the AC side, because BESS can achieve multiple functions with that position. The DC link voltage involves the quality of PWM control for the grid-side VSC, which may require additional energy storage, especially for the WEC system.

V. Conclusion

This paper proposes a WEC power conversion system with GFM control, utilizing six PMLGs to replace the hydraulic system in TALOS as the PTO. The GFM control facilitates the integration of the WEC system into the AC grid, providing capabilities for frequency response and voltage support. The findings indicate that the BESS on the DC link effectively smooths the power output of the PMLGs, delivers additional power for frequency response, and stabilizes the DC link voltage. Comparative analysis of the WEC system's operation under MPPT mode and constant power mode reveals that constant power mode demands more power from the BESS. This insight is crucial for designing the capacity of the BESS. With consideration of both smoothing power output of PMLGs and providing frequency support, this study formulates a calculation equation for accurately sizing the peak power of BESS. A comparison between different locations of BESS has been presented as well, which shows the DC link could be in a better position for BESS when compared to the placement at the AC side. There are also some future work in improving the performance of WEC system with BESS at AC link. Specially designed VSG control can help the WEC system track accurately under MPPT mode. In addition, the battery sizing only focuses on the peak power of the battery. Future research will aim to design an optimal energy management system for BESS considering the SoC.

Acknowledgements

The authors wish to thank the financial support for the research work by the EPSRC funding support (Grant No. EP/V040561/1) for the project ‘Novel High-Performance Wave Energy Converters with advanced control, reliability and survivability systems through machine-learning forecasting (NHP-WEC)’ for the TALOS WEC project.

References

[1] “Renewable energy targets”, European Commission, 2023, online: https://energy.ec.europa.eu/topics/renewable-energy/renewable-energy-directive-targets-and-rules/renewable-energy-targets_en

[2] C. Hall, W. Sheng, Y. Wu, G. Aggidis, “The impact of model predictive control structures and constraints on a wave energy converter with hydraulic power take off system” in *Renewable Energy*, vol. 224, 2024.

[3] G.A. Aggidis, C.J. Taylor, "Overview of wave energy converter devices and the development of a new multi-axis laboratory prototype", IFAC-PapersOnLine, vol. 50, 2017, pp. 15651-15656.

[4] W. Sheng, E. Tapoglou, X. Ma, CJ Taylor, R. Dorrell, DR Parsons and G. Aggidis, “Time-Domain Implementation and Analyses of Multi-Motion Modes of Floating Structures. *Journal of Marine Science and Engineering*, 2022

[5] Jusoh, M.A.; Ibrahim, M.Z.; Daud, M.Z.; Albani, A.; Mohd Yusop, Z. “Hydraulic Power Take-Off Concepts for Wave Energy Conversion System: A Review”, in *Energies*, 2019.

[6] I. López, J. Andreu, S. Ceballos, I. M. de Alegría, I. Kortabarria, "Review of wave energy technologies and the necessary power-equipment", in *Renewable and Sustainable Energy Reviews*, vol. 27, pp. 413-434, 2013.

[7] Faiz, J. and Nematsaberi, A. “Linear electrical generator topologies for direct-drive marine wave energy conversion- an overview”. *IET Renewable Power Generation*, pp. 1163-1176, 2017

[8] R. Datta and V. T. Ranganathan, "Variable-speed wind power generation using doubly fed wound rotor induction machine-a comparison with alternative schemes," in *IEEE Transactions on Energy Conversion*, vol. 17, no. 3, pp. 414-421, Sept. 2002.

[9] EirGrid Group. “EirGrid Grid Code”, 2021, version 10, [Online] Available:https://www.eirgridgroup.com/site-files/library/EirGrid/GridCodeVersion10.pdf

[10] A.J. Hillis, C. Whitlam, A. Brask, J. Chapman, A.R. Plummer, "Active control for multi-degree-of-freedom wave energy converters with load limiting", in *Renewable Energy*, vol. 159, pp. 1177-1187,2020.

[11] M. Jama, A. Wahyudie and S. Mekhilef, "Wave Excitation Force Estimation Using an Electrical-Based Extended Kalman Filter for Point Absorber Wave Energy Converters," in *IEEE Access*, vol. 8, pp. 49823-49836, 2020.

[12] H. A. Said, D. García-Violini, J. V. Ringwood, "Wave-to-grid (W2G) control of a wave energy converter", Energy Conversion and Management: X, vol. 14, 2022

[13] F. Wu, X. P. Zhang, P. Ju and M. J. H. Sterling, "Optimal Control for AWS-Based Wave Energy Conversion System," in *IEEE Transactions on Power Systems*, vol. 24, no. 4, pp. 1747-1755, Nov. 2009.

[14] G. Rajapakse, S. Jayasinghe, A.Fleming, M. Negnevitsky, "Grid Integration and Power Smoothing of an Oscillating Water Column Wave Energy Converter". in *Energies*, 2018.

[15] M. Talaat, Bishoy E. Sedhom, and A.Y. Hatata, “A new approach for integrating wave energy to the grid by an efficient control system for maximum power based on different optimization techniques”, *International Journal of Electrical Power & Energy Systems*, vol. 128, 2021.

[16] Ullah, M.I., Döhler, J.S., de Albuquerque, V.M., Forslund, J., Boström, C., and Temiz, I. “Multi-mode converter control for linear generator-based wave energy system”. *IET Renew. Power Gener*. 1–15, 2024.

[17] M. Trapanese, V. Boscaino, G. Cipriani, D. Curto, V. D. Dio and V. Franzitta, "A Permanent Magnet Linear Generator for the Enhancement of the Reliability of a Wave Energy Conversion System," in *IEEE Transactions on Industrial Electronics*, vol. 66, no. 6, pp. 4934-4944, June 2019.

[18] H. -P. Beck and R. Hesse, "Virtual synchronous machine," *2007 9th International Conference on Electrical Power Quality and Utilisation*, Barcelona, Spain, 2007, pp. 1-6.

[19] S. D’Arco, J. A. Suul, O. B. Fosso, “A Virtual Synchronous Machine implementation for distributed control of power converters in SmartGrids” in *Electric Power Systems Research*, vol.122, pp. 180-197, 2015.

[20] F. Shahnia, "Impact of low pass filters of the droop control on converter-interfaced DERs of an islanded microgrid," *2016 IEEE International Conference on Industrial Technology (ICIT)*, Taipei, Taiwan, 2016, pp. 317-322.

[21] A. Yazdani and R. Iravani, Voltage-Sourced Converters in Power System, New York, NY, USA: Wiley-IEEE Press, Mar. 2010.